



Supplement of

Impact of 2020 COVID-19 lockdowns on particulate air pollution across Europe

Jean-Philippe Putaud et al.

Correspondence to: Jean-Philippe Putaud (jean.putaud@ec.europa.eu)

The copyright of individual parts of the supplement might differ from the article licence.

Table S1. Regulated air pollutant measurement methods employed at urban sites.

Site	PM ₁₀	PM _{2.5}	NO	NO ₂	O ₃
Helsinki	on-line microbalance	on-line microbalance	chemiluminescence	chemiluminescence_ Mo converter	UV absorption
Oslo	optical particle counting	optical particle counting	chemiluminescence	chemiluminescence_ Mo converter	UV absorption
Copenhagen	on-line microbalance	on-line microbalance	chemiluminescence	chemiluminescence_ Mo converter	UV absorption
Rotterdam	β -attenuation	β -attenuation	chemiluminescence	chemiluminescence_ Mo converter	UV absorption
Leipzig	on-line microbalance	N/A	chemiluminescence	chemiluminescence_ Mo converter	UV absorption
Brussels	on-line microbalance ⁽¹⁾	on-line microbalance ⁽¹⁾	chemiluminescence	chemiluminescence_ Mo converter	UV absorption
Lille	on-line microbalance ⁽¹⁾	on-line microbalance ⁽¹⁾	chemiluminescence	chemiluminescence_ Mo converter	UV absorption
Prague	β -attenuation	β -attenuation	chemiluminescence	chemiluminescence_ photolytic converter	UV absorption
Paris	on-line microbalance ⁽¹⁾	N/A	chemiluminescence	chemiluminescence_ Mo converter	UV absorption
Bern	gravimetric	gravimetric	chemiluminescence	chemiluminescence_ Mo converter	UV absorption
Milan	β -attenuation	N/A	chemiluminescence	chemiluminescence_ Mo converter	UV absorption
Barcelona	gravimetric	gravimetric	chemiluminescence	chemiluminescence_ Mo converter	UV absorption
Athens	gravimetric	gravimetric	chemiluminescence	chemiluminescence_ Mo converter	UV absorption
Seville	β -attenuation	N/A	chemiluminescence	chemiluminescence_ Mo converter	UV absorption
Granada	β -attenuation	N/A	chemiluminescence	chemiluminescence_ Mo converter	UV absorption
Nicosia	on-line microbalance ⁽¹⁾	on-line microbalance ⁽¹⁾	chemiluminescence	chemiluminescence_ photolytic converter	UV absorption

(1) with Filter Dynamic Measurement System[®]

Table S2. Regulated air pollutant measurement methods employed at regional background sites.

Site	PM ₁₀	PM _{2.5}	NO	NO ₂	O ₃
HYY	gravimetric	gravimetric	chemiluminescence	chemiluminescence_ Mo converter	UV absorption
BIR	gravimetric	gravimetric	chemiluminescence	iodide impregnated glass sinter	UV absorption
RIS	gravimetric	gravimetric	chemiluminescence	chemiluminescence_ Mo converter	UV absorption
CBW	β-attenuation	β-attenuation	chemiluminescence	chemiluminescence_ Mo converter	UV absorption
MEL	gravimetric	gravimetric	chemiluminescence	chemiluminescence_ Mo converter	UV absorption
KOS	gravimetric	gravimetric	chemiluminescence	chemiluminescence_ photolytic converter	UV absorption
SIR	optical particle counting	optical particle counting	chemiluminescence	chemiluminescence_ photolytic converter	UV absorption
PAY	gravimetric	gravimetric	chemiluminescence	chemiluminescence_ Mo converter	UV absorption
IPR	on-line microbalance ⁽¹⁾	N/A	chemiluminescence	chemiluminescence_ photolytic converter	UV absorption
MSY	gravimetric	gravimetric	chemiluminescence	chemiluminescence_ Mo converter	UV absorption
ARN	β-attenuation	N/A	chemiluminescence	chemiluminescence_ Mo converter	UV absorption
CYP	gravimetric	gravimetric	chemiluminescence	chemiluminescence_ photolytic converter	UV absorption

(1) with Filter Dynamic Measurement System[®]

Table S3. Multi-wavelength aerosol light absorption and particle number size distribution instruments employed at urban and regional background sites.

Site	Time period	multi-WL light absorption ¹⁾		particle number size distribution		
		instrument type ¹⁾	WL range (nm)	instrument type ²⁾	lower bound (nm)	upper bound (nm)
Helsinki	2017-2020	N/A	N/A	DMPS	3	794
Oslo	2017-2020	AE33	370 - 950	N/A	N/A	N/A
Copenhagen	2017-2020	N/A	N/A	SMPS	40	478
Rotterdam	2019-2020	N/A	N/A	N/A	N/A	N/A
Leipzig	2017-2020	N/A	N/A	SMPS	10	800
Brussels	2017-2020	AE31	370 - 950	N/A	N/A	N/A
Lille	2017-2020	AE33	370 - 950	SMPS	16	800
Bern	2018-2020	AE33 ³⁾	370 - 950	N/A	N/A	N/A
Milan	2019-2020	N/A	N/A	N/A	N/A	N/A
Barcelona	2017-2020	AE33	370 - 950	SMPS	11	478
Athens	2017-2020	AE33	370 - 950	SMPS	10	550
Granada	2017-2020	N/A	N/A	SMPS	11	496
Nicosia	2017-2020	AE33	370 - 950	N/A	N/A	N/A
HYY	2017-2020	CLAP	467 - 652	DMPS	3	1000
BIR	2017-2020	PSAP	470 - 660	DMPS	10	800
RIS	2017-2020	N/A	N/A	SMPS	40	478
MEL	2017-2020	N/A	N/A	SMPS	5	800
KOS	2017-2020	AE33	470 - 660	SMPS	9	845
SIR	2017-2020	AE33	370 - 950	N/A	N/A	N/A
PAY	2017-2020	AE33	370 - 950	N/A	N/A	N/A
IPR	2017-2020	AE31	370 - 950	DMPS	10	800
MSY	2017-2020	AE33	370 - 950	SMPS	9	856
ARN	2019-2020	CLAP	467 - 652	SMPS	14	673

1: AE = aethalometer[®], CLAP = continuous light absorption photometer, PSAP = particle soot absorption photometer

2: DMPS = differential mobility particle sizer, SMPS = scanning mobility particle sizer

3: AE31 until November 2018

Table S4. Coefficients of determination of the linear regression between daily CAMS ensemble forecast and observation data in February-May 2019 across the sites considered in this study. Coefficients ≥ 0.5 (1 significant digit) in bold.

	NO ₂	NO	O ₃	PM ₁₀	PM _{2.5}
Helsinki	0.46	0.25	0.32	0.29	0.54
Oslo	0.46	0.49	0.67	0.13	0.56
Copenhagen	0.46	0.23	0.61	0.63	0.68
Rotterdam	0.70	0.85	0.79	0.63	0.77
Leipzig	0.78	0.63	0.65	0.73	N/A
Brussels	0.77	0.64	0.66	0.80	0.80
Lille	0.58	0.38	0.75	0.74	0.80
Prague	0.54	0.48	0.61	0.65	0.64
Paris	0.72	0.76	0.75	0.73	N/A
Bern	0.64	0.57	0.71	0.59	0.54
Milan	0.73	0.82	0.82	0.71	N/A
Barcelona	0.56	0.58	0.78	0.53	0.58
Athens	0.29	0.34	0.17	0.36	0.62
Seville	0.47	N/A	0.41	0.50	N/A
Granada	0.56	0.40	0.68	0.37	0.07
Nicosia	0.38	0.24	0.58	0.49	0.36
HYY	0.81	0.35	0.43	0.37	0.50
BIR	0.11	N/A	0.56	0.61	0.74
RIS	0.60	0.27	0.42	0.60	0.67
CBW	0.83	0.77	0.81	0.63	0.71
MEL	0.81	0.69	0.65	0.59	0.65
KOS	0.57	0.45	0.47	0.70	0.68
SIR	0.75	0.66	0.63	0.77	0.76
PAY	0.72	0.56	0.64	0.61	N/A
IPR	0.66	0.57	0.75	0.63	N/A
MSY	0.47	0.13	0.43	0.33	0.29
ARN	0.61	N/A	0.77	0.00	N/A
CYP	0.20	0.06	0.44	0.66	0.41

Table S5. Regressions between national monthly road fuel consumption (source: EUROSTAT) and monthly mean driving direction request (source: Apple®) indices for the time period January – May 2020. Fuel consumption and driving direction request data are normalised to January 2020 and 13 January 2020 data, respectively.

	gasoline			diesel		
	slope	slope relative uncertainty	R ²	slope	slope relative uncertainty	R ²
Finland	0.49	41%	0.66	-0.36	37%	0.71
Norway	0.42	44%	0.63	0.05	280%	0.04
Denmark	0.53	67%	0.43	-0.41	59%	0.49
Netherlands	0.70	19%	0.90	-0.67	56%	0.51
Germany	0.48	33%	0.76	-0.19	105%	0.23
Belgium	0.88	23%	0.86	-0.03	936%	0.00
France	0.80	23%	0.86	0.39	33%	0.76
Czech Republic	0.38	50%	0.57	0.17	100%	0.25
Switzerland ⁽¹⁾	0.59	25%	0.84	0.18	95%	0.27
Italy	0.52	18%	0.91	0.44	13%	0.95
Spain	0.71	13%	0.95	0.37	24%	0.85
Greece	0.59	20%	0.89	-0.07	240%	0.05

(1) Source for fuel consumption: www.avenergy.ch

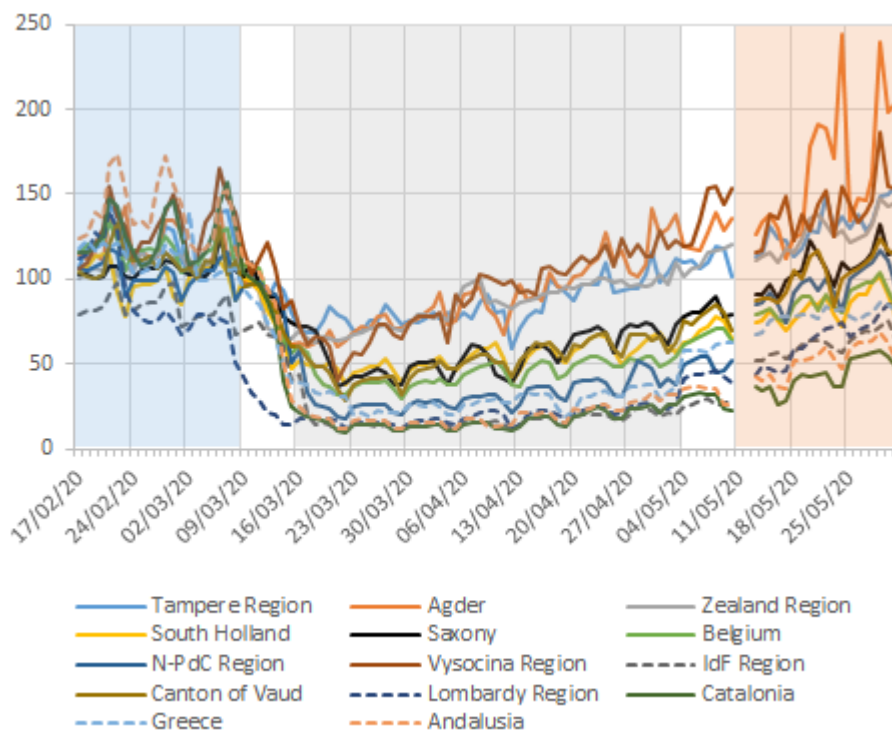
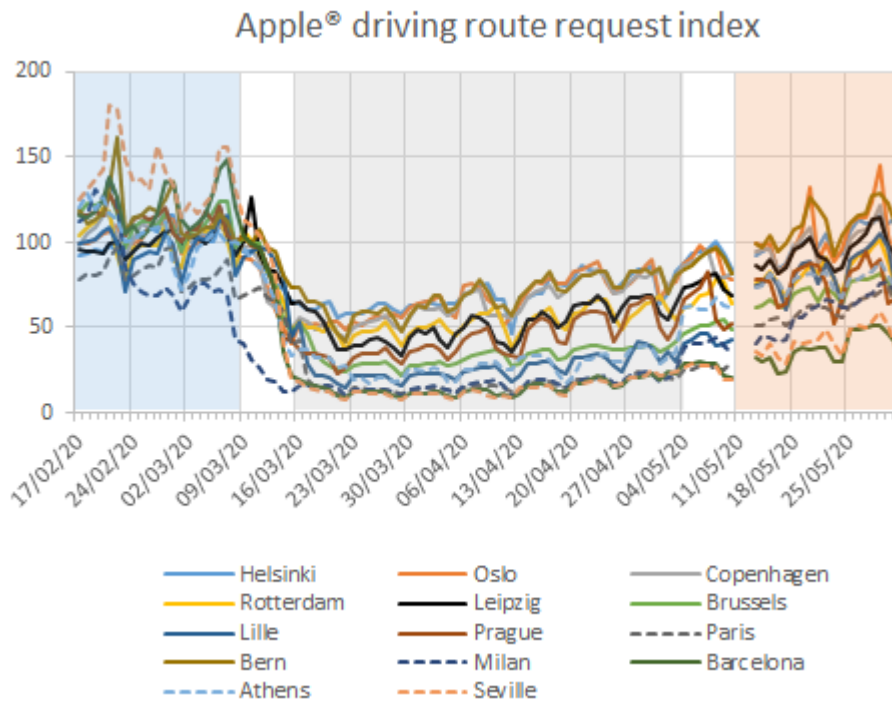


Figure S1: driving route request index from Apple® in cities and regions of the study. The 3 periods A (before), D (during) and P (after lockdown) are highlighted by the light blue, grey, and orange backgrounds, respectively.

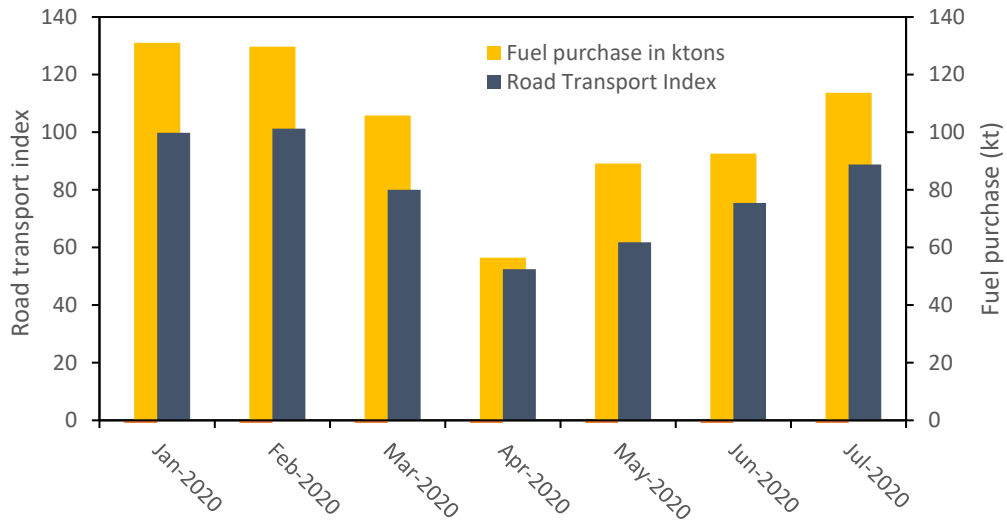


Figure S2. 2020 mobility and fuel purchase data from Cyprus (source: //library.cystat.gov.cy/NEW/MONTH-ECON_IND-TABLE1A1B-JANDEC21-EL-140222.xls). Road transport index 2015 = 100. Fuel purchase is that of oil companies.

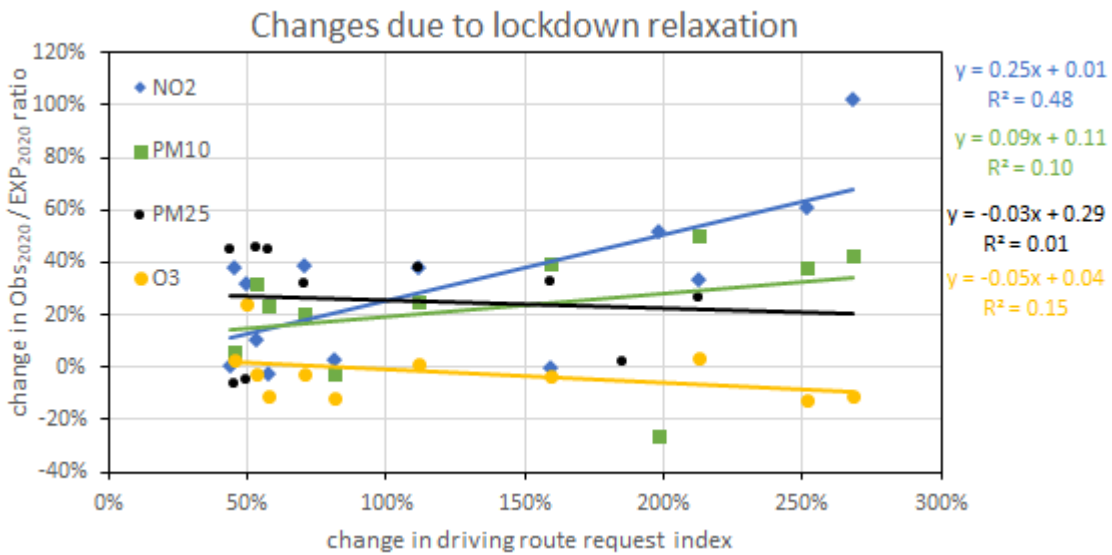
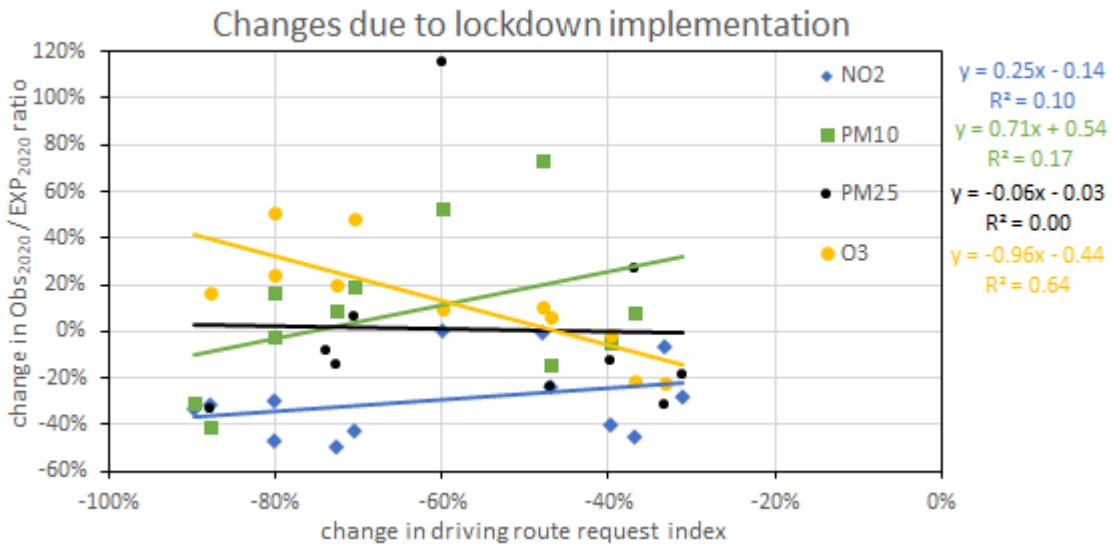


Figure S3. Regressions between changes in observed / expected concentration ratios and driving route request index at urban sites between A and D (top) and between D and P (bottom).

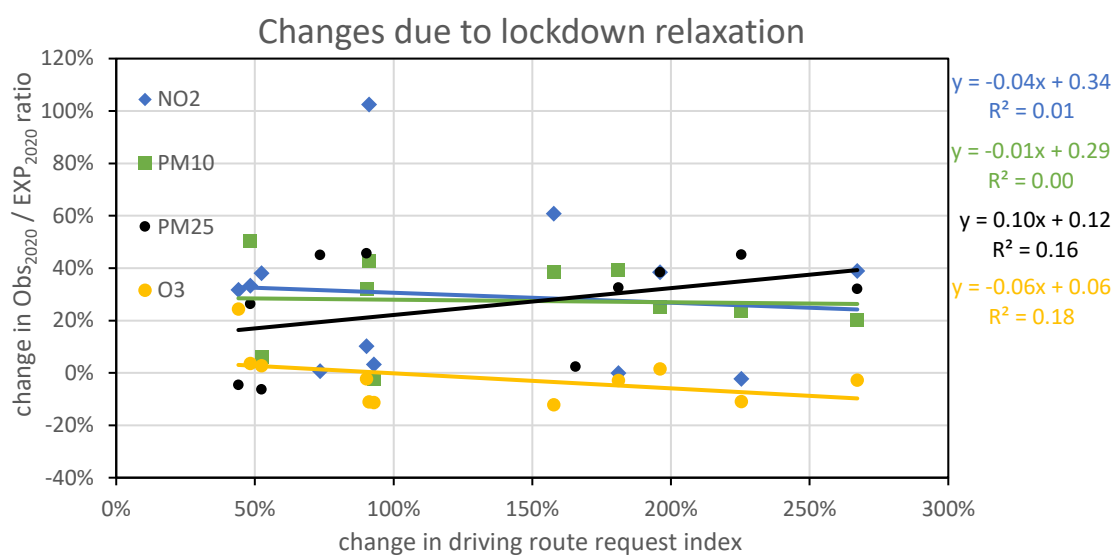
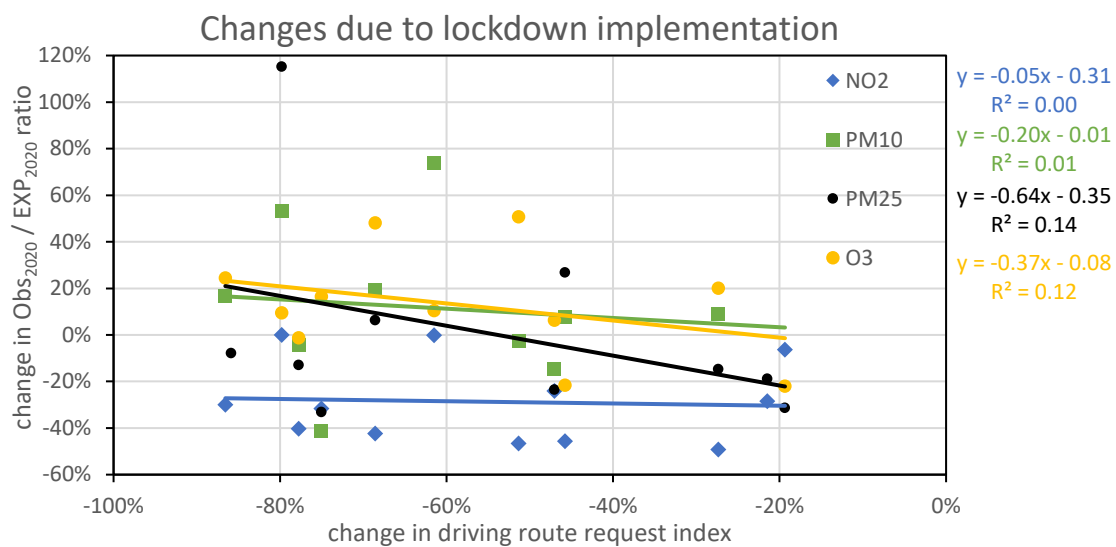


Figure S4. Regressions between changes in observed / expected concentration ratios and driving route request index at regional background sites between A and D (top) and between D and P (bottom).

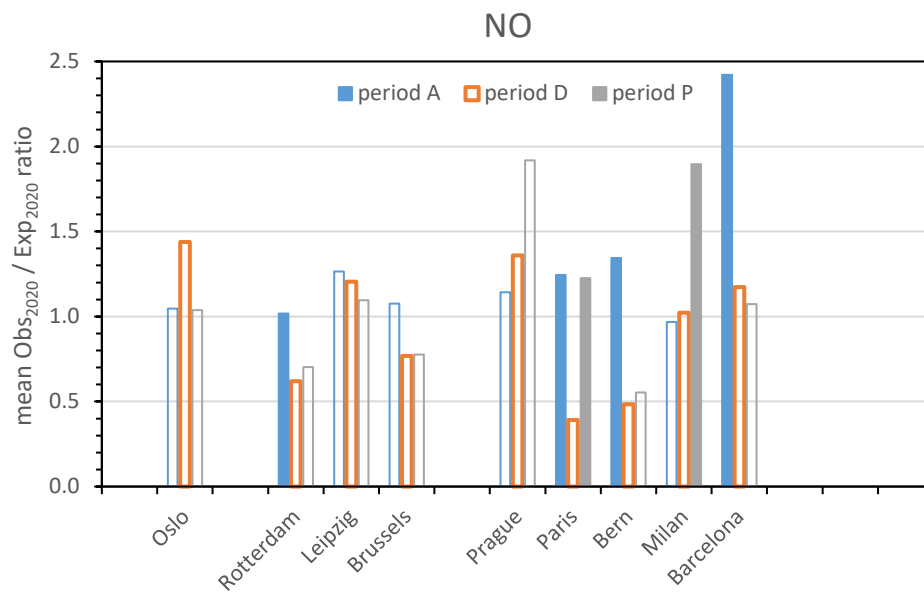


Figure S5. Mean observed / expected NO concentration ratios at urban sites before (A), during (D) and after (P) the lockdown period. Filled bars indicate means which are statistically different from the mean during lockdown period (D) at the 95% confidence level.

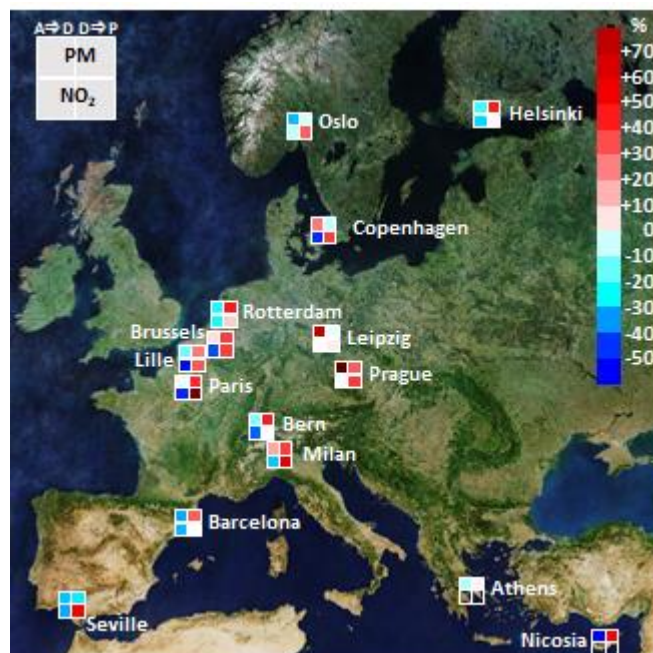


Figure S6: Impacts of lockdown implementations (A⇌D) and relaxations (D⇌P) on PM and NO₂ concentrations at 15 urban sites considered in our study. When available (see Table S1), PM_{2.5} data are shown. Map background from ESA.